Subwavelength Target Detection Using Ultrawideband Time-Reversal Techniques With a Multilayered Dielectric Slab

Tien-Hao Liao, Po-Chuan Hsieh, and Fu-Chiarng Chen, *Member, IEEE*

***Abstract*—We employed a multilayered dielectric slab to implement subwavelength target detection by utilizing ultrawideband (UWB) time-reversal (TR) techniques. Simulation results with/without the multilayered dielectric slab are presented to show the benefit of the multilayered dielectric slab structure using finite-difference time-domain (FDTD) method.**

***Index Terms*—Finite-difference time-domain (FDTD), multilayered dielectric slab, time-reversal (TR), ultrawideband (UWB).**

I. Introduction

TIME-REVERSAL (TR) techniques exploit the temporal reversibility characteristic of wave equations [1]. TR techniques in acoustics have shown much potential for many applications, such as underwater acoustic communication [2], medical imaging, destruction of kidney stones, and nondestructive detection [3]. Moreover, TR techniques employing EM waves are considered beneficial for applications of wireless communication since EM waves have the advantages of polarization diversity, good penetration ability, and faster wave velocity [4], [5].

For nondestructive target-detection methodologies, we may encounter two main problems. The first is to break the diffraction limit to resolve targets, namely, how fine we can distinguish the targets. The second problem is that the intervening media variation scenario shows impacts on target information. More seriously, signals traveling back from target(s) may be weak and distorted by intervening media variation scenarios.

Compared to other nondestructive methodologies, electromagnetic ultrawideband (UWB) signals exploit their wideband advantage in TR techniques to improve the detection capabilities [6]–[8]. However, the intervening media variation scenario, which produces the multiple scattering effect, is an unpredictable factor for detection performance either numerically or experimentally. For example, we may find that either a random forest of parallel steel rods or a continuous random medium is employed to create the scattering-rich environment to achieve subwavelength focusing effects [9], [10]. Those strategies offer multiple scattering performances randomly. Randomly distributed scatterers may vary with time in real-world scenarios, so the performances of TR techniques may also vary with the changing scattering conditions rather than have predictable performances.

In this letter, we propose the utilization of multilayered dielectric slab to improve the retrofocusing resolution of TR techniques with UWB signals. The multilayered dielectric slab can create the multiple scattering effect in the predictable manner instead of a time-varying one. The whole investigation is realized with finite-difference time-domain (FDTD) method [11], where the numerical simulation setup is introduced in the third section. Simulation results are presented to investigate how the subwavelength retrofocusing phenomenon can be reached using the multilayered dielectric slab.

II. Multilayered Dielectric Slab

For TR techniques, multiple scattering effect plays the role of assisting TR techniques in improving the focusing ability, and therefore becomes a popular topic in recent years [9], [10], [12]. We propose a new kind of structure called the multilayered dielectric slab, shown in Fig. 1. As its name infers, the structure is composed of 16 dielectric layers, each of which contains two neighbor-value dielectric constants in the iterative order, and the average dielectric constant of the slab distributes itself increasingly from its center to both sides.

The multilayered dielectric slab plays the role of enlarging the receiver aperture width, which is defined as the effective receiver array size. With larger receiver aperture width, the channel information can be collected more completely. There are two means of producing larger receiver aperture width; the first is to increase the effective aperture size of the array by adding receiver elements, and the second is to increase the information each receiver element can collect using the fixed number of array elements. Compared to actually increasing the effective aperture size of the array, the second one is considered a more economical solution, and our proposed structure of the multilayered dielectric slab can meet this purpose. Fig. 2 explains how the multilayered dielectric slab enlarges the receiver aperture width. Fig. 2(a) and (b) show that two waves in different directions have the chance to reach the same receiver either in line-of-sight (LOS) or non-line-of-sight (NLOS) paths, and the signal may diversify its paths into different receivers

Manuscript received March 30, 2009. First published June 23, 2009; current version published July 28, 2009. This work was supported by the National Science Council of Taiwan under Contract NSC 95-2221-E-009-044-MY3 and by the Ministry of Education (MOE) Aiming for the Top University (ATU) and Elite Research Center Development Plan.

The authors are with the Department of Communication Engineering, National Chiao Tung University, Hsinchu, Taiwan (e-mail: fchen@faculty.nctu.edu.tw).

Color versions of one or more of the figures in this letter are available online at http://ieeexplore.ieee.org.

Digital Object Identifier 10.1109/LAWP.2009.2025897

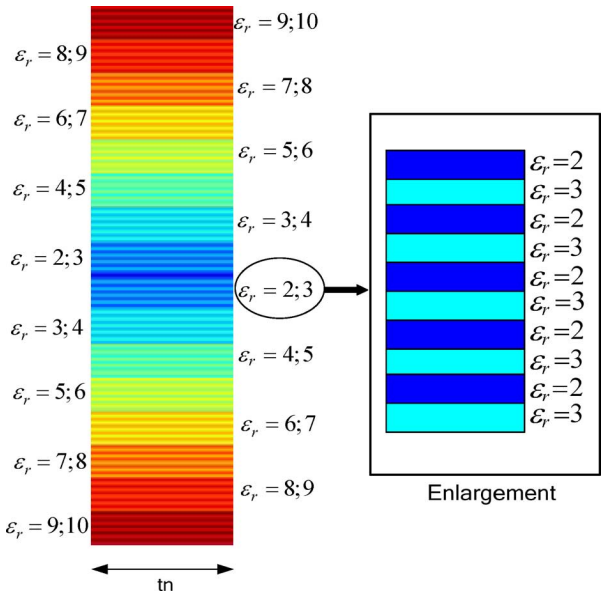

Fig. 1. The design of multilayered dielectric slab. The width of the slab is tn, and the values of dielectric constants range from 2 to 10.

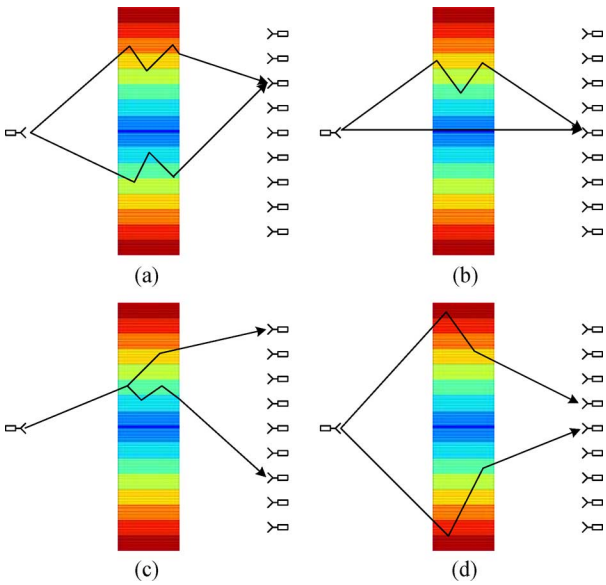

Fig. 2. Possible propagation routes in the inhomogeneous environment that is created by the multilayered dielectric slab.

once penetrating through the slab in Fig. 2(c). Fig. 2(d) explains that the signals, originally impossibly received by the receivers of the central part, now can arrive at the receivers of the central part with the addition of the multilayered dielectric slab. Therefore, the multilayered dielectric slab can enlarge the receiver aperture width with limited receiver elements.

A more important benefit of the multilayered dielectric slab is that it can create the multiple scattering effect in a more predictable manner to improve the resolution. Previous works like [9] and [10] mostly tend to utilize the random characteristics of multiple scattering both numerically and experimentally. Randomly distributed scatterers may vary with time in real-world scenarios, so the performances of TR techniques may also vary

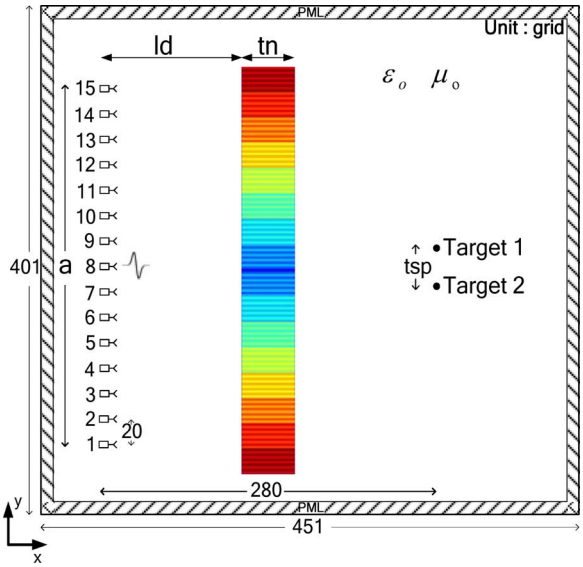

Fig. 3. Illustration of FDTD simulation setup. The transceiver array elements are numbered in series from 1 to 15, and the physical array size is a. The distance between the transceiver array and multilayered dielectric slab is ld, while the slab width is tn, which is fixed at 40 mesh grids. Especially, tsp is the distance between two targets.

with the ever-changing scattering conditions. If an artificially scattering-rich environment can be created, the performance of TR techniques can be kept more predictable rather than environmentally dependent and time-varying, and thus beneficial for target detection.

For the design of the multilayered dielectric slab, the dielectric constants of the central part of the slab are set to be close to that of the free space. The central elements of the transceiver array receive most power directly reflecting back from the targets and, therefore, still keep the retrofocusing phenomenon at the stronger power level. Second, the dielectric constant of the slab distributes itself increasingly from its center to both sides, and this design ensures that the waves traveling obliquely into the slab result in more refraction effect and thus diversify the propagating routes to different transceivers. Moreover, the iterative dielectric distribution of the multilayered dielectric slab can help the incident waves create more multiple scattering to carry more information from targets. The abovementioned phenomena are predictable operations because of employing the proposed multilayered dielectric slab and, therefore, approve the multilayered dielectric slab for utilizing multiple scattering in a more predictable manner. We will present the simulation results in the fourth section to reveal the benefit of the multilayered dielectric slab.

III. Computational Setup

TM wave is implemented in our simulation for simplicity of observation. We choose the Gaussian monopulse with the central frequency $(\mathrm{f_c})$ 6.85 GHz as the UWB excitation, and the size of spatial mesh grids $(\triangle \mathrm{s})$ and the size of time-steps $(\triangle \mathrm{t})$ can be determined to be 1 mm and 1 ps, respectively [11]. Fig. 3 shows the numerical setup of TR simulation with two PEC targets whose radii are both 2 mm. The size of simulation domain is 451×401 mesh grids, and 10 layers of PML are surrounded to

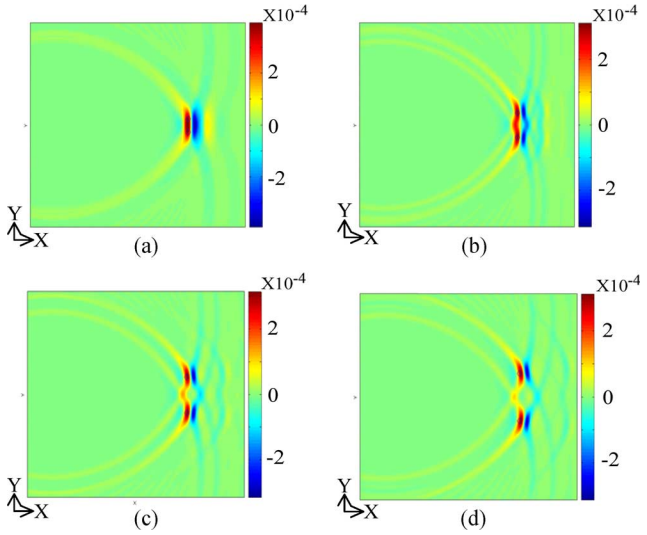

Fig. 4. Simulation results of time-reversed $\mathrm{E_Z}$ field of two-target detection at the time of retrofocusing. (a), (b), (c), and (d) are simulations in homogeneous space where the distance between two targets (tsp) is 22, 44, 66, and 88 grids.

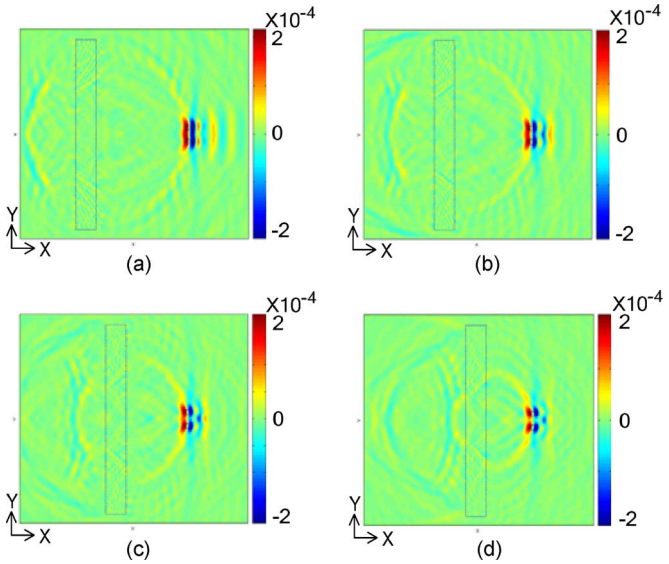

Fig. 5. Simulation results of time-reversed $\mathrm{E_Z}$-field of two-target detection at the time of retrofocusing. (a), (b), (c), and (d) are simulations with the multilayered dielectric slab where the distance between the transceiver array and multilayered dielectric slab (ld) is 60, 90, 120, and 150 grids.

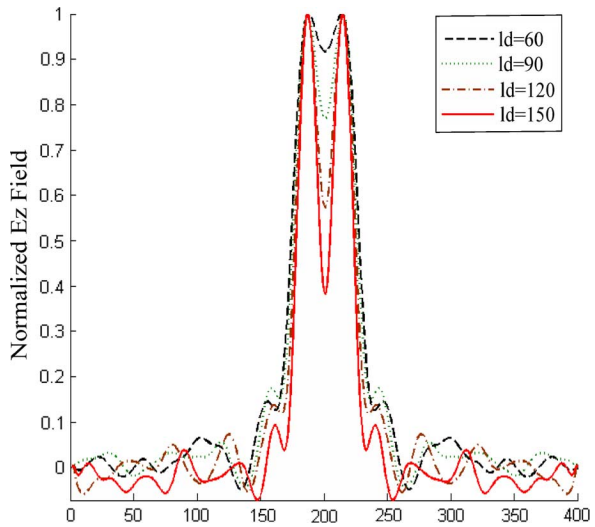

Fig. 6. Normalized $\mathrm{E_Z}$-field results for the simulation in Fig. 5 at $\mathrm{x} = 330$ with respect to y-coordinate.

ensure the simulation domain extended to infinity [13]. A 15-element transceiver array parallel to the y-axis is implemented with physical array size (a) 280 grids. The distance between the transceiver array and targets is fixed at 280 grids.

The whole TR simulation process is described as follows. First, the eighth element of the transceiver array emits the UWB signal into the simulation domain. The UWB signal first penetrates through the multilayered dielectric slab. Once encountering the PEC target(s), waves reflect backward, again penetrate through the slab, and are finally recorded by 15 transceiver elements. The second step is to time-reverse the scattered waveforms and re-emit them into the simulation domain.

IV. Computational Result

A. Two-Target Detection in Homogeneous Space

We first simulate the case of two-target detection numerically in the homogeneous space, namely free space, as the reference case. The varying parameter of this first case is the distance between two targets (tsp), which ranges from 22 to 88 grids. The simulation results are plotted in Fig. 4.

In Fig. 4(a), tsp is 22 grids $(= 0.5\lambda_c)$, so the time-reversed signals cannot retrofocus on the location of the two closely-spaced targets distinctly. In contrast, as two targets get farther, we may find the time-reversed signals can detect the existence of two PEC targets as shown in Fig. 4(b)–(d).

B. Two-Target Detection With Multilayered Dielectric Slab

Similar simulation setups are performed with addition of the multilayered dielectric slab as shown in Fig. 3. Two PEC targets are located at $(\mathrm{x}, \mathrm{y}) = (330, 189)$ and (330,211), where tsp is 22 grids $(= 0.5\lambda_c)$ in the simulation domain, the distance at which the time-reversed signals cannot retrofocus in the free space. The distance between the transceiver array and the multilayered dielectric slab (ld), from 60 to 150 grids, is varied as a parameter to investigate how the multilayered dielectric slab helps improve retrofocusing performances. Figs. 5 and 6 present the results where we snapshot the $\mathrm{E_Z}$-field distribution at the moment of the strongest retrofocusing, and the maximum value of the $\mathrm{E_Z}$ is normalized to 1 V/m along $\mathrm{x} = 330$ in Fig. 6. What draws our attention is when ld gets larger, the resolution becomes better.

When the slab is close to the transceiver array, signals emitted from the array mostly penetrate through the center of the slab. Smaller ld only makes the retrofocusing phenomenon keep at the stronger power level, but makes little use of the multipath effect that the multilayered dielectric slab offers. In contrast, when the slab is farther from the transceiver array, the signals can penetrate the whole slab. As the signals spread to the end-sides of the slab, more signals can diversify their paths, making good use of the structure of the multilayered dielectric slab. The transceiver aperture width can be enlarged equivalently and help

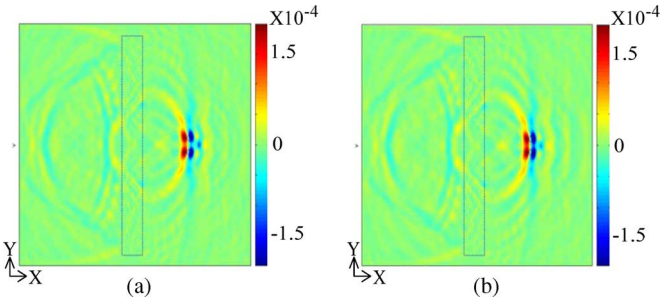

Fig. 7. Simulation results of time-reversed E_Z field of two-target detection at the time of retrofocusing where the distance between two targets (tsp) is (a) 20 and (b) 18 grids.

reach the resolution enhancement. It thus becomes realizable to distinguish the existence of two targets where their distance is as close as 22 grids $(= 0.5\lambda_c)$, shown in Fig. 6.

Furthermore, we examine how fine the resolution can be reached by shortening the distance between two targets (tsp) as well. The distance between the transceiver array and the multilayered dielectric slab (ld) is still fixed at 150 grids, but we reduce tsp from 22 grids to 20 and 18 grids, which means tsp is less than half a wavelength. The results are shown in Fig. 7, and we may observe when tsp is reduced to 18 grids, which is $0.4\lambda_c$ wide, the retrofocusing phenomenon can still achieve good resolution to detect the existence of two neighboring objects. This indicates that the proposed multilayered dielectric slab indeed helps achieve the phenomenon for subwavelength target detection.

V. Conclusion

In this work, we investigate how to reach subwavelength target detection with our proposed multilayered dielectric slab. It is proved numerically that the multilayered dielectric slab offers a predictable multiple scattering effect for target detection using UWB time-reversal techniques. Future study is needed on the structure optimization of our proposed multilayered dielectric slab for subwavelength target-detection applications.

References

[1] M. Fink, "Time-reversed acoustics," *Sci. Amer.*, pp. 91–97, Nov. 1999.
[2] G. F. Edelmann, T. Akal, W. S. Hodgkiss, S. Kim, W. A. Kuperman, and H. C. Song, "An initial demonstration of underwater acoustic communication using time reversal," *IEEE J. Ocean. Eng.*, vol. 27, no. 3, pp. 602–609, Jul. 2002.
[3] N. Chakroun, M. A. Fink, and F. Wu, "Time reversal processing in ultrasonic nondestructive testing," *IEEE Trans. Ultrason., Ferroelectr., Freq. Control*, vol. 42, no. 6, pp. 1087–1097, Feb. 1995.
[4] H. T. Nguyen, J. B. Andersen, and G. F. Pedersen, "The potential use of time reversal techniques in multiple element antenna systems," *IEEE Commun. Lett.*, vol. 9, no. 1, pp. 40–42, Jan. 2005.
[5] B. E. Henty and D. D. Stancil, "Multipath-enabled super-resolution for RF and microwave communication using Phase-Conjugate Arrays," *Phys. Rev. Lett.*, vol. 93, p. 243904, 2004.
[6] M. Fink, D. Cassereau, A. Derode, C. Prada, P. Roux, M. Tanter, J. Thomas, and F. Wu, "Time-reversed acoustics," *Rep. Prog. Phys.*, vol. 63, pp. 1933–1995, 2000.
[7] F.-C. Chen and W. C. Chew, "Experimental verification of super-resolution in nonlinear inverse scattering," *Appl. Phys. Lett*, vol. 72, pp. 3080–3082, 1998.
[8] F.-C. Chen and W. C. Chew, "Time-domain ultra-wideband imaging radar experiment for verifying super-resolution in nonlinear inverse scattering," *J. Electromagn. Waves Appl.*, vol. 17, no. 9, pp. 1243–1260, 2003.
[9] A. Derode, A. Tourin, J. de Rosny, M. Tanter, S. Yon, and M. Fink, "Taking advantage of multiple scattering to communicate with time-reversal antennas," *Phys. Rev. Lett.*, vol. 90, p. 014301, 2003.
[10] M. E. Yavuz and F. L. Teixeira, "A numerical study of time reversed UWB electromagnetic waves in continuous random media," *IEEE Antennas Wireless Propag. Lett.*, vol. 4, pp. 43–46, 2005.
[11] A. Taflove, *Computational Electrodynamics: The Finite-Difference Time-Domain Method*. Norwood, MA: Artech House, 1995.
[12] G. Lerosey, J. de Rosny, A. Tourin, A. Derode, G. Montaldo, and M. Fink, "Time reversal of electromagnetic waves," *Phys. Rev. Lett.*, vol. 92, no. 19, p. 193904, 2004.
[13] J. P. Berenger, "A perfectly matched layer for the absorption of electromagnetic waves," *J. Comput. Phys.*, vol. 114, pp. 185–200, 1994.